Altered nitric oxide production mediates matrix-specific PAK2 and NF-κB activation by flow

Arif Yurdagul, Jr.[a,b], Jie Chen[a], Steven Daniel Funk[a,b], Patrick Albert[a], Christopher G. Kevil[a,b], and A. Wayne Orr[a,b]
Departments of [a]Pathology and [b]Cell Biology and Anatomy, LSU Health Sciences Center, Shreveport, LA 71103

ABSTRACT Shear stress generated by distinct blood flow patterns modulates endothelial cell phenotype to spatially restrict atherosclerotic plaque development. Signaling through p21-activated kinase (PAK) mediates several of the deleterious effects of shear stress, including enhanced NF-κB activation and proinflammatory gene expression. Whereas shear stress activates PAK in endothelial cells on a fibronectin matrix, basement membrane proteins limit shear-induced PAK activation and inflammation through a protein kinase A–dependent pathway; however, the mechanisms underlying this regulation were unknown. We show that basement membrane proteins limit membrane recruitment of PAK2, the dominant isoform in endothelial cells, by blocking its interaction with the adaptor protein Nck. This uncoupling response requires protein kinase A–dependent nitric oxide production and subsequent PAK2 phosphorylation on Ser-20 in the Nck-binding domain. Of importance, shear stress does not stimulate nitric oxide production in endothelial cells on fibronectin, resulting in enhanced PAK activation, NF-κB phosphorylation, ICAM-1 expression, and monocyte adhesion. These data demonstrate that differential flow–induced nitric oxide production regulates matrix-specific PAK signaling and describe a novel mechanism of nitric oxide–dependent NF-κB inhibition.

INTRODUCTION

Atherosclerotic plaques form preferentially in regions of disturbed blood flow, such as arterial curvatures, branch points, and bifurcations. Endothelial cells sense frictional shear stress generated by blood flow and convert these forces into intracellular biochemical signals that regulate endothelial cell function (Hahn and Schwartz, 2009). Models of disturbed flow, such as low flow or oscillatory flow, promote endothelial permeability, activate the proinflammatory transcription factor NF-κB, and induce the expression of proinflam-

matory proteins involved in monocyte recruitment, such as ICAM-1 and VCAM-1 (Hahn and Schwartz, 2009). In contrast to disturbed flow, prolonged laminar flow generated in relatively straight regions of the vasculature stimulates production of the vasodilator nitric oxide (NO) and concomitantly reduces endothelial permeability and proinflammatory gene expression (Hahn and Schwartz, 2009; Andrews et al., 2010). In addition to vasodilation, NO can limit NF-κB activation and block leukocyte adhesion to the endothelium, indicating that shear stress–induced NO production suppresses atherogenic endothelial activation (De Caterina et al., 1995; Khan et al., 1996). Of interest, endothelial cells show similar initial responses to laminar and disturbed flow, including both NF-κB activation and proinflammatory gene expression (Hahn and Schwartz, 2009; Chiu and Chien, 2012). However, laminar flow abrogates these proinflammatory responses at later times as the cells adapt and align to laminar flow. In contrast, disturbed flow does not cause endothelial alignment and induces the sustained activation of proinflammatory responses, suggesting that disparate cellular adaptation to flow may underlie the differential inflammatory response (Orr et al., 2005; Hahn and Schwartz, 2009).

The p21-activated kinase (PAK) family of Ser/Thr kinases mediates several of the endothelial cell responses to shear. Shear stress

activates PAK signaling in endothelial cells in culture, and regions of disturbed flow in vivo show elevated levels of PAK activation concomitant with enhanced proinflammatory gene expression and initiation of atherogenesis (Orr *et al.*, 2007; Funk *et al.*, 2010). Inhibiting PAK signaling blunts endothelial permeability (Orr *et al.*, 2007), JNK and NF-κB activation (Orr *et al.*, 2008; Hahn *et al.*, 2009), and proinflammatory gene expression (Orr *et al.*, 2008) both in response to shear stress in vitro and at sites of disturbed flow in apolipoprotein E (ApoE)–knockout mice in vivo. Taken together, these data suggest a central role for PAK signaling in shear stress–induced endothelial cell activation and early atherogenesis.

Shear stress activates PAK through the integrin family of extracellular matrix receptors (Funk *et al.*, 2010). However, integrin-specific signaling on different extracellular matrix proteins profoundly affects this response. On transitional matrix proteins such as fibronectin and fibrinogen, shear stress promotes PAK signaling, NF-κB activation, and ICAM-1/VCAM-1 expression (Orr *et al.*, 2005, 2007, 2008). On basement membrane proteins (collagen IV, laminin), shear stress activates protein kinase A (PKA), which suppresses PAK and NF-κB activation (Orr *et al.*, 2005, 2007, 2008). Transitional matrix deposition occurs early during atherogenesis in vivo concomitant with endothelial cell proinflammatory responses (Orr *et al.*, 2005), and preventing fibronectin matrix assembly with peptide inhibitors can blunt endothelial ICAM-1 and VCAM-1 expression in carotid ligation models (Chiang *et al.*, 2009). Furthermore, genetic deletion of plasma fibronectin in ApoE-deficient mice reduces PAK and NF-κB activation as well as ICAM-1 expression at sites of disturbed flow, thereby hindering early atherosclerotic plaque formation (Rohwedder *et al.*, 2012).

The mechanisms mediating matrix-specific PAK activation remain poorly understood. Activation of group 1 PAK isoforms (PAK1/2/3) involves both membrane targeting and relief of autoinhibition by small GTPases (Lu *et al.*, 1997; Lu and Mayer, 1999). The scaffolding protein Nck recruits PAK to the plasma membrane by binding a proline-rich region in the N-terminus of PAK (Lu *et al.*, 1997). At the plasma membrane, interaction with active GTP-bound Rac and cdc42 relieves the autoinhibition and stimulates PAK autophosphorylation in the kinase domain and autoinhibitory domain, resulting in PAK activation (Bokoch, 2003). Whereas Rac is required for shear stress–induced PAK activation, shear stress–induced Rac activation is similar on basement membrane proteins and transitional matrices (Funk *et al.*, 2010). Cells in suspension limit PAK activation by blocking the PAK–Nck interaction (Howe, 2001), but this mode of PAK regulation has not been demonstrated in adherent cells. Thus we sought to determine whether basement membrane proteins affect the PAK–Nck interaction to limit shear stress–induced endothelial cell activation and analyze the role of PKA in this response.

RESULTS

Matrix regulates PAK/Nck association and PAK targeting to cell membrane

To determine how PAK activation is regulated, we first characterized which group 1 PAK isoforms are expressed in macrovascular endothelial cells. Both protein and mRNA analysis show that PAK2 is the dominant class 1 PAK isoform expressed in human aortic, coronary artery, and umbilical vein endothelial cells, as well as in bovine aortic endothelial cells (Supplemental Figure S1, A and B). To test whether matrix composition affects PAK2 membrane targeting, we exposed endothelial cells plated on basement membrane proteins or the transitional matrix protein fibronectin to shear stress and assessed PAK2 translocation to the membrane fraction. Whereas

fibronectin supports shear stress–induced PAK2 membrane targeting, endothelial cells on basement membrane proteins showed no shear-induced PAK2 translocation to the membrane (Figure 1A). Consistent with an important role for Nck in PAK2 membrane translocation, shear stress significantly enhanced the interaction between PAK and Nck in endothelial cells on fibronectin but not in cells on basement membrane proteins as determined by coimmunoprecipitation (Figure 1B).

The Nck-binding proline-rich sequence in the N-terminal regulatory domain of PAK contains several putative phosphorylation sites. Because phosphorylation of Ser-21 in PAK1 abrogates the interaction of PAK and Nck (Zhao *et al.*, 2000), we hypothesized that shear stress–induced signaling on basement membrane proteins prevents the PAK–Nck interaction through enhanced phosphorylation within the Nck-binding domain. To test this, we analyzed whether matrix composition affected shear stress–induced PAK2 phosphorylation on Ser-20, analogous to the Ser-21 site on PAK1. Consistent with reduced Nck binding, shear stress stimulated PAK2 Ser-20 phosphorylation on basement membrane proteins but not on fibronectin (Figure 1C). Similarly, endothelial cells exposed to 18 h of oscillatory flow showed enhanced PAK2 Ser-20 phosphorylation on basement membrane proteins compared with fibronectin (Figure 1D and Supplemental Figure S1C). To verify the inhibitory nature of PAK2 Ser-20 phosphorylation, we created a PAK2 S20A point mutant that lacks the ability to be phosphorylated on Ser-20. Expression of PAK2 S20A rescued shear stress–induced PAK2 activation (Ser-141 phosphorylation) in endothelial cells on basement membrane proteins, whereas wild-type PAK2 did not (Figure 1E).

Shear stress induces PKA-dependent PAK2 serine 20 phosphorylation on basement membrane proteins

Previous results demonstrated that PKA signaling was required to limit shear-induced PAK activation on basement membrane proteins (Funk *et al.*, 2010). Therefore we next characterized PKA's role in shear stress–induced PAK2 Ser-20 phosphorylation. Consistent with PKA-dependent PAK2 inhibition, treatment with the PKA inhibitors PKI and H89 significantly blunted shear-induced Ser-20 phosphorylation (Figure 2A and Supplemental Figure S2A). Knockdown of the PKA Cα catalytic domain (75% knockdown; Supplemental Figure S2B) rescued shear stress–induced PAK2 activation on basement membrane proteins (Funk *et al.*, 2010) and significantly blunted shear-induced PAK2 Ser-20 phosphorylation (Figure 2B). Whereas PKA inhibition (PKI) enhanced shear stress–induced PAK2 activation (Figure 2C and Supplemental Figure S2C), this rescue was completely abrogated by blocking the PAK–Nck interaction with membrane-permeable peptide corresponding to the Nck-binding sequence of PAK. Taken together, these data suggest that enhanced shear stress–induced PKA activation on basement membrane proteins promotes PAK2 Ser-20 phosphorylation, thereby limiting PAK activation.

Although PKA is required for shear-induced PAK2 Ser-20 phosphorylation, PKA could stimulate Ser-20 phosphorylation either directly or indirectly through other downstream signaling mediators. PKA can directly phosphorylate PAK1 in nonadherent cells on an undetermined site (Howe and Juliano, 2000), but a similar phosphorylation of PAK2 has not yet been demonstrated. Therefore we expressed a recombinant multiepitope-tagged PAK2 construct in endothelial cells, immunoprecipitated recombinant PAK2, and performed an in vitro kinase assay using recombinant active PKA. Western blotting for phosphorylated PKA substrate sequences (RXXpT or RRXpS) illustrated an increase in PAK2 phosphorylation that was completely inhibited by the PKA inhibitor PKI, demonstrating that PKA does phosphorylate PAK2 directly in
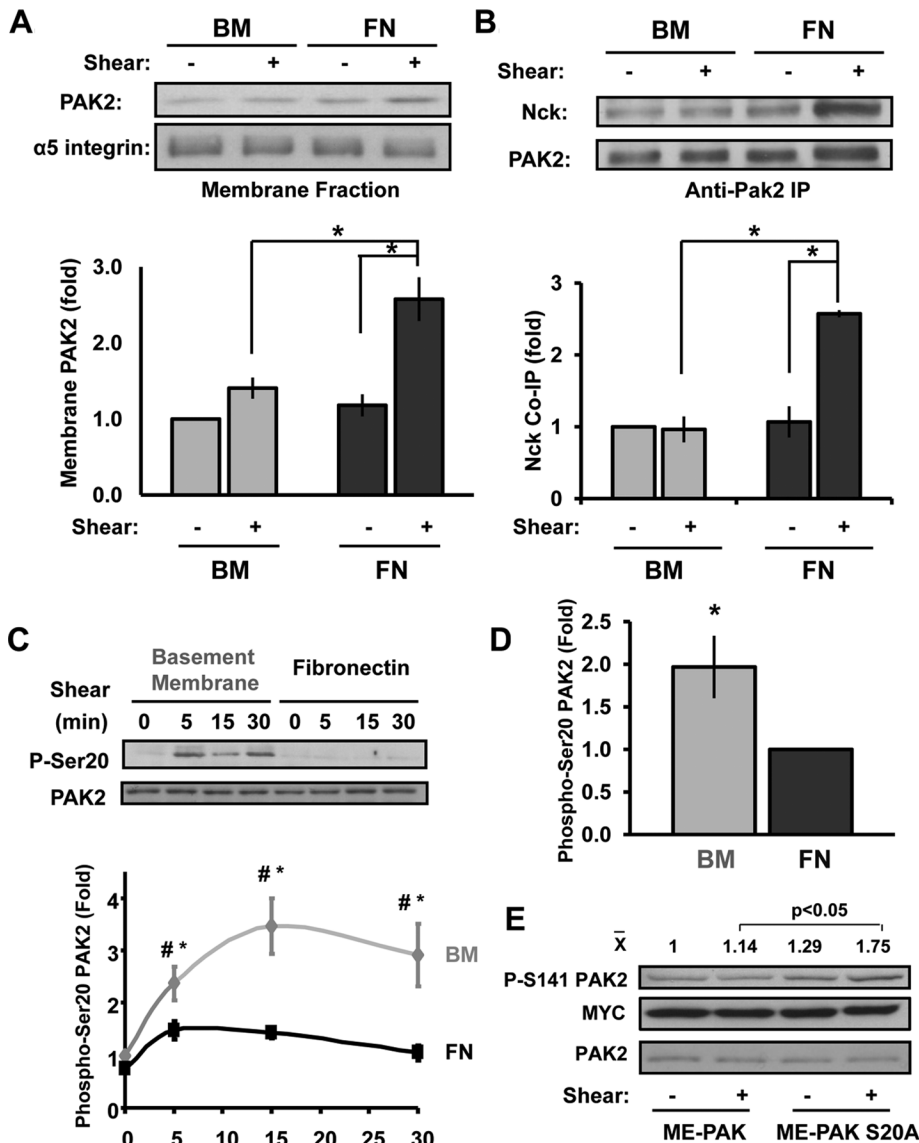
FIGURE 1: Matrix controls Nck-dependent PAK2 membrane targeting through PAK2 Ser-20 phosphorylation. (A) BAECs on basement membrane proteins (BM) or fibronectin (FN) were sheared for 15 min, and PAK2 levels in cytosolic and membrane fractions were analyzed by Western blotting. Results are normalized to α5 integrin levels in the membrane fraction. Representative immunoblots are shown. $n = 3$. (B) Coimmunoprecipitation of Nck in PAK2 immunoprecipitates was determined by Western blotting and normalized to PAK2 levels in the pull downs. Representative immunoblots are shown. $n = 3$ (C) Endothelial cells on BM or FN were sheared for the indicated times, and Ser-20 phosphorylation was determined by immunoblotting. Values are means ± SE, $n = 3$. *$p < 0.05$ compared with static condition, #$p < 0.05$ comparing matrices. (D) HAECs plated on either BM or FN were exposed to oscillatory shear stress (OSS) for 18 h, and Ser-20 phosphorylation was determined as in C. Values are means ± SE, $n = 4$. (E) BAECs expressing a multiepitope (ME)-tagged PAK2 construct or a S20A mutant were plated on basement membrane proteins and sheared for 30 min. PAK2 phosphorylation on Ser-141 corresponding to PAK activation was then assessed by Western blotting. Representative blots and mean densitometry values for PAK Ser-141 phosphorylation are shown. $n = 3$. *$p < 0.05$.

Basement membrane proteins enhance shear-induced NO production through PKA

PKA signaling is implicated in shear stress–induced NO production (Boo *et al.*, 2002a), and the NO-activated kinase protein kinase G (PKG) can phosphorylate the homologous Ser-21 site on PAK1 (Fryer *et al.*, 2006). Therefore, whereas PKA is capable of phosphorylating Ser-20 directly, PKA may mediate Ser-20 phosphorylation in intact cells through the downstream activation of NO/PKG signaling. To test this, we next assessed whether matrix composition affects shear stress–induced NO production. Endothelial cells on different matrix proteins were exposed to shear stress for 2 h, and total NO species production was determined using a Sievers NO analyzer. Of interest, shear stress significantly stimulated NO production in endothelial cells plated on basement membrane proteins but not in cells on fibronectin (Figure 3A). A similar matrix-specific NO production was also observed when endothelial cells were treated with long-term (18 h) laminar or oscillatory flow (Figure 3B), demonstrating that matrix composition significantly affects the ability of shear stress to induce NO production. The diminished NO production in cells on fibronectin is not due to decreased endothelial NO synthase (eNOS) expression, as fibronectin enhanced eNOS expression after chronic laminar and oscillatory flow (Supplemental Figure S4A).

Shear stress promotes NO production in part through eNOS phosphorylation on several residues including Ser-1179 (Dimmeler *et al.*, 1999; Fulton *et al.*, 1999) and Ser-635 (Boo *et al.*, 2002a, 2003). Consistent with matrix-specific NO production, shear stress induced eNOS Ser1179 (Figure 3, C and D) and Ser-635 phosphorylation (Figure 3, C and E) specifically in endothelial cells on basement membrane proteins. In addition, eNOS phosphorylation on Thr-497 reduces NO production (Chen *et al.*, 1999b), and endothelial cells on fibronectin show enhanced shear-induced phosphorylation of the inhibitory Thr-497 site, consistent with decreased eNOS activity (Figure 3, D and G).

Published reports suggested that PKA signaling drives shear-induced eNOS phosphorylation on both Ser-635 and Ser-1179 (Boo *et al.*, 2002a,b), and basement membrane proteins promote both shear stress–induced PKA activation (Funk *et al.*, 2010) and NO production (Figure 3, A and B). Consistent with these studies, the PKA inhibitors PKI and H89 were both sufficient to block shear stress–induced NO production (Figure 4A) and eNOS Ser1179 phosphorylation (Figure 4B) in endothelial cells on basement membrane proteins. However, PKA inhibitors did not block Ser-635 phosphorylation and even elevated Ser-635 phosphorylation under static

in vitro kinase assays (Supplemental Figure S3A). Furthermore, the residues surrounding PAK Ser-20 (RMSS²⁰T) are similar to consensus PKA phosphorylation sites (RRXS and RXXT), and Western blotting with phospho–Ser-20 antibodies demonstrated a strong increase in PAK2 Ser-20 phosphorylation after PKA-mediated phosphorylation (Supplemental Figure S3B).
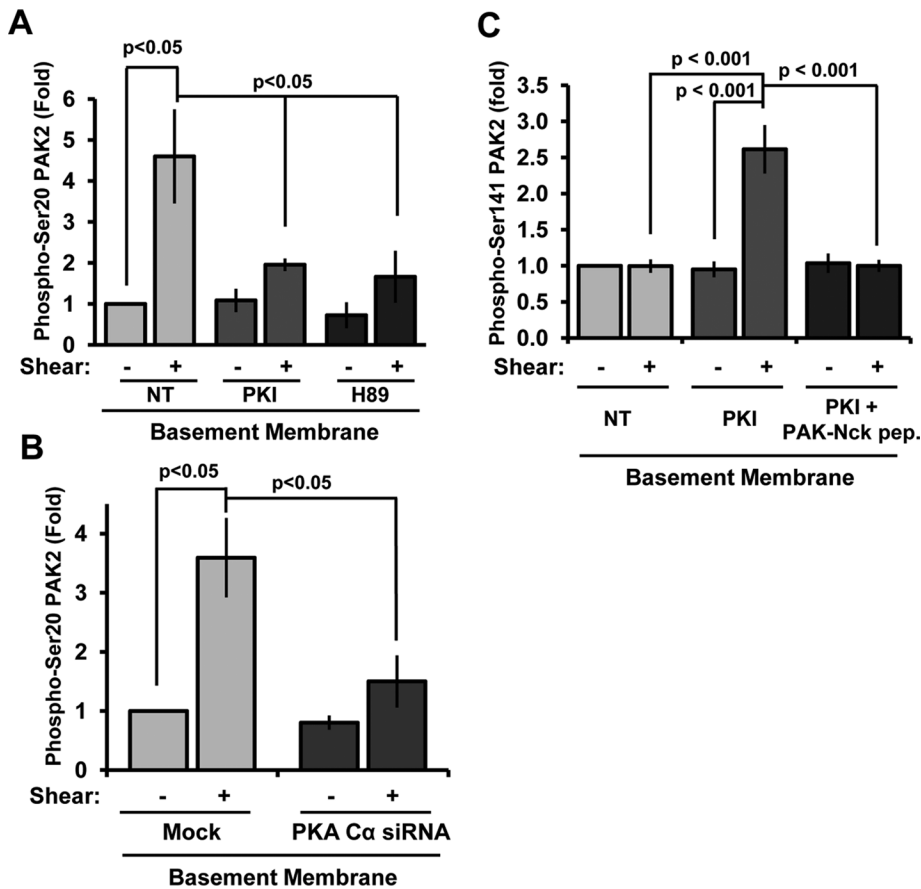
A

B

C

FIGURE 2: Shear stress–induced PAK2 Ser-20 phosphorylation is PKA dependent. (A) BAECs were treated with the PKA inhibitor PKI (20 µM) or H89 (5 µM) for 30 min before application of fluid shear stress (15 min), and Ser-20 phosphorylation was determined by immunoblotting. Values are means ± SE, $n = 3$. (B) Endothelial cells transfected with siRNA against PKA Cα were sheared for 15 min, and Ser-20 phosphorylation was determined. Values are means ± SE, $n = 3$. (C) Endothelial cells were treated with PKI (20 µM) in the absence or presence of the PAK–Nck blocking peptide (20 µg/ml), and shear stress-induced PAK2 activation was determined by Western blotting as previously described. $n = 3$.

brane proteins (Figure 5D) but did not affect shear stress–induced PKA activation (Figure 5E). Therefore, although PKA can phosphorylate PAK2 Ser-20 directly in vitro, PKA activation is not sufficient for shear stress–induced PAK2 Ser-20 phosphorylation on basement membrane proteins and instead requires downstream PKA-dependent NO/PKG signaling. Taken together, these data suggest that enhanced shear-induced NO/PKG signaling on basement membrane proteins drives Ser-20 phosphorylation, thereby reducing PAK2 membrane translocation.

PAK Ser-20 phosphorylation mediates the anti-inflammatory effect of NO/PKG signaling

PAK2 critically mediates shear stress–induced NF-κB activation and proinflammatory gene expression, and a peptide inhibitor of the PAK–Nck interaction is sufficient to block shear-induced NF-κB activation in both in vitro and in vivo model systems (Orr *et al.*, 2008). Given that blocking the NO/PKG pathway blunts Ser-20 phosphorylation and rescues PAK activation, we next asked whether endothelial cells on basement membrane proteins use the NO/PKG pathway to block PAK-dependent NF-κB activation. Addition of NO/PKG inhibitors (CPTIO, ODQ, KT5823) was sufficient to rescue shear stress–induced NF-κB activation in cells on basement membrane proteins (Figure 6A and Supplemental Figure S5B). siRNA-mediated eNOS knockdown similarly rescued shear stress–induced NF-κB activation (Figure 6B), suggesting that enhanced NO/PKG signaling on basement membrane pro-

teins blunts proinflammatory signaling to NF-κB. Consistent with this concept, preventing PAK2 Ser-20 phosphorylation directly by transfecting endothelial cells with the PAK2 S20A mutant restored shear stress–induced NF-κB activation in cells on basement membrane proteins (Figure 6C). Moreover, activation of PKG signaling with the cell-permeable cGMP analogue 8-CPT cGMP was sufficient to inhibit shear-induced NF-κB activation in endothelial cells on fibronectin (Figure 6D), underscoring the importance of the NO/PKG pathway in the matrix-specific response to shear stress.

To further confirm that PKG prevents NF-κB activation by blocking the PAK-Nck interaction, we treated endothelial cells on basement membrane proteins with the PKG inhibitor KT5823 in the absence or presence of the membrane-permeable PAK–Nck blocking peptide. The enhanced shear stress–induced NF-κB activation in cells treated with PKG inhibitors was completely blocked by competing away the PAK-Nck interaction (Figure 7A). In addition, enhanced shear-induced ICAM-1 expression after PKG inhibition was similarly abrogated by the PAK–Nck peptide (Figure 7B), suggesting that KT5823 rescues NF-κB activity by promoting the PAK–Nck interaction. To verify that proinflammatory responses are altered under these conditions, we performed monocyte adhesion assays in human aortic endothelial cell (HAECs) treated with KT5823 and the PAK–Nck peptide before stimulation with shear stress. Consistent

conditions (Supplemental Figure S4B). Together these data demonstrate that matrix-specific PKA signaling critically regulates shear stress–induced eNOS phosphorylation on Ser-1179 to control NO production.

NO/PKG signaling is required for PAK2 inhibition on basement membrane proteins

To determine whether enhanced NO-dependent PKG signaling mediates PAK2 Ser-20 phosphorylation on basement membrane proteins, we next assayed whether inhibitors of NO/PKG signaling could blunt shear-induced PAK2 Ser-20 phosphorylation. The NO scavenger 2-4-carboxyphenyl-4,4,5,5-tetramethylimidazoline-1-oxyl-3-oxide (CPTIO), the guanylate cyclase inhibitor 1H-[1,2,4]oxadi-azolo[4,3-a]quinoxalin-1-one (ODQ), and the PKG inhibitor KT-5823 were all sufficient to blunt shear-induced PAK2 Ser-20 phosphorylation (Figure 5A and Supplemental Figure S5A) and rescue PAK activation (Ser-141 phosphorylation; Figure 5B and Supplemental Figure S5A) in endothelial cells on basement membrane proteins. Consistent with the pharmacological inhibitor data, small interfering RNA (siRNA)–mediated eNOS knockdown also significantly blunted shear stress–induced PAK2 Ser-20 phosphorylation (Figure 5C). Furthermore, inhibiting PKG signaling with KT-5823 rescued shear stress–induced PAK2 membrane translocation on basement mem-
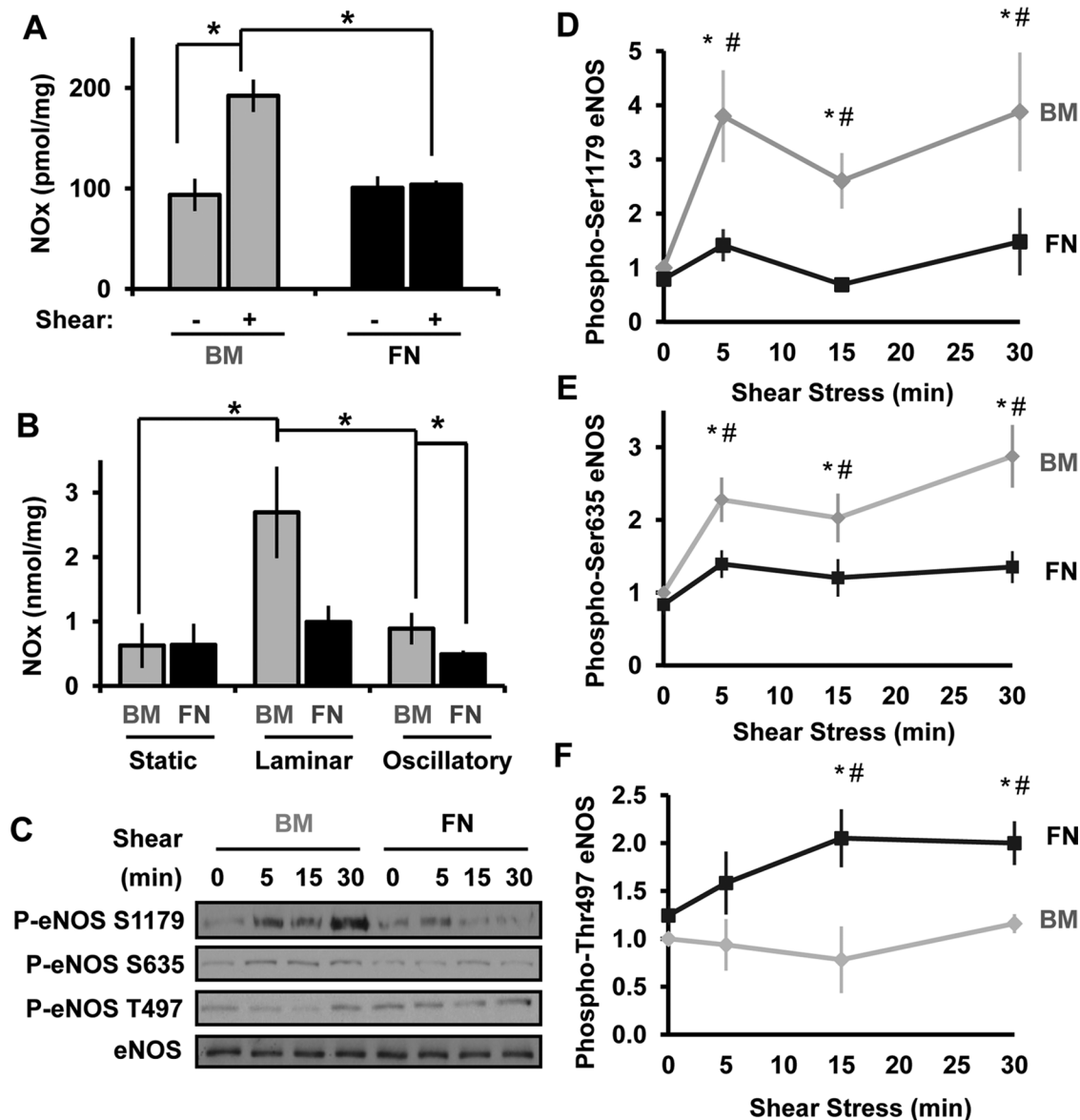
FIGURE 3: Basement membrane proteins promote flow-induced NO production. (A) BAECs on BM or FN were exposed to shear stress for 2 h, and NO species (NOx) were quantified using the Sievers NO analyzer via chemiluminescence and normalized to total protein levels in the lysates. $n = 3$. (B), Endothelial cells on BM or FN were subjected laminar shear stress (LSS) or oscillatory shear stress (OSS) for 18 h or maintained under static conditions. NOx levels were measured as described in A. $n = 3$. (C–F) Endothelial cells on either BM or FN were sheared for the indicated times, and eNOS phosphorylation on Ser-1179, Ser-635, and Thr-497 was determined by Western blotting. Results were normalized to GAPDH, and values shown are means ± SE. Representative images are shown in C. $n = 3$. *$p < 0.05$ compared with static, #$p < 0.05$ compared between matrices.

with signaling and gene expression data, adhesion of THP-1 monocytes was significantly enhanced in KT5823-treated cells exposed to shear stress (Figure 7, C and D), and this enhanced adhesion was completely repressed by pretreating cells with the PAK–Nck inhibitory peptide. Taken together, these data demonstrate that PKG regulates shear stress–induced NF-κB activation by controlling the interaction between PAK2 and Nck.

DISCUSSION
These data strongly support the hypothesis that matrix remodeling plays a major role in endothelial cell activation during early atherogenesis. Previous work demonstrated that basement membrane proteins actively suppress shear stress–induced endothelial cell acti-

vation through PKA-dependent PAK inhibition (Funk *et al.*, 2010). In this work, we demonstrate that PKA accomplishes this by inhibiting PAK membrane targeting through NO/PKG-dependent PAK2 Ser-20 phosphorylation. In addition, we demonstrate that shear stress does not significantly stimulate NO production in endothelial cells plated on the transitional fibronectin matrix resulting in enhanced activation of PAK and NF-κB. These data illustrate a novel role for matrix composition in shear stress–induced NO production and identify a novel anti-inflammatory mechanism of NO/PKG signaling by inhibiting the PAK–Nck interaction and PAK-dependent NF-κB activation (Figure 8).

The interaction between PAK and Nck has long been associated with PAK activation. Membrane targeting of Nck's second SH3
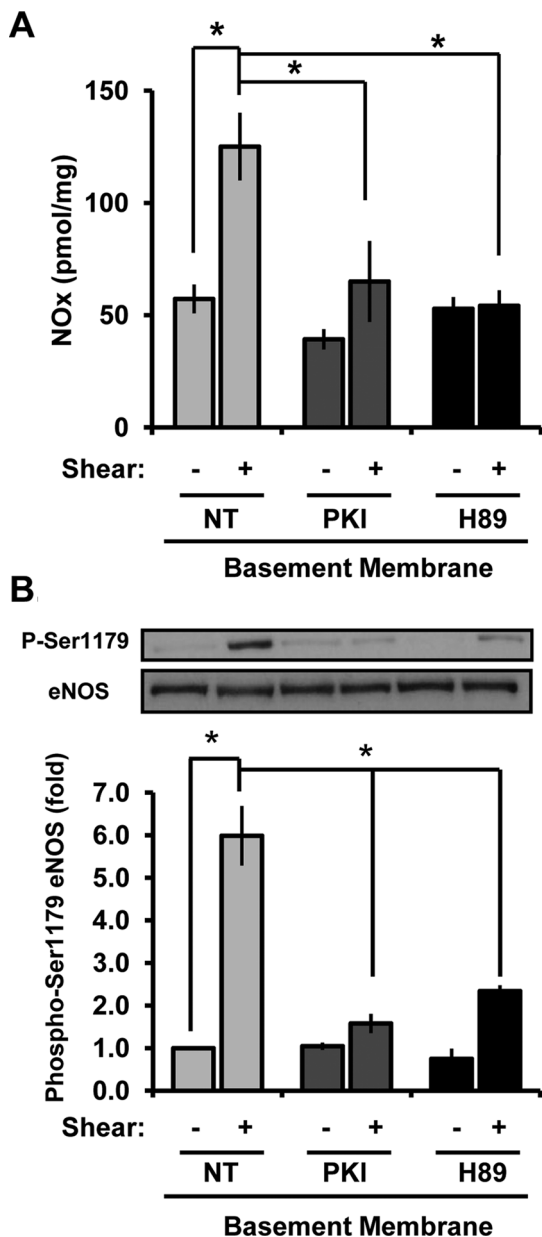
FIGURE 4: Enhanced NO production on basement membrane proteins is PKA dependent. (A) BAECs on BM were treated with PKI (20 µM, 15 min) or H89 (5 µM, 30 min) and sheared for 2 h, and NOx levels in cell lysates were determined using the Sievers NO analyzer via chemiluminescence and normalized to total protein levels in the lysates. $n = 3$. $*p < 0.05$. (B) Endothelial cells were treated as in A and sheared for 30 min. eNOS phosphorylation on Ser-1179 was determined by Western blotting. Results were normalized to total eNOS, and values shown are means ± SE. $n = 3$. $*p < 0.05$.

domain stimulates PAK activation directly through a Rho GTPase-dependent pathway (Lu *et al.*, 1997; Lu and Mayer, 1999), suggesting that efficient PAK activation requires both membrane translocation (Nck dependent) and relief of autoinhibition (Rac/cdc42 dependent). However, data suggesting PAK activation can be regulated at the level of Nck binding are limited. PAK inactivation in cells in suspension is associated with reduced PAK–Nck interactions and enhanced PAK phosphorylation near the Nck-binding site (Howe, 2001). Whereas PAK2 Ser-20 phosphorylation is a site of weak

autophosphorylation (Zhan *et al.*, 2003; Zhou *et al.*, 2003), phosphorylation at this site is more strongly induced by Akt and PKG, resulting in PAK detargeting out of focal adhesions (Zhou *et al.*, 2003; Fryer *et al.*, 2006). Therefore the transphosphorylation of inactive PAK by other kinases may limit its Nck-dependent targeting to the plasma membrane and prevent its activation. Furthermore, inhibiting the PAK–Nck interaction is sufficient to reduce NF-κB activation and vascular permeability at sites of disturbed flow (Orr *et al.*, 2007, 2008), suggesting that the intrinsic regulation of PAK–Nck interactions by intracellular signaling pathways may serve to limit PAK-associated endothelial cell activation in vivo. Whereas loss of the PAK–Nck interaction is known to contribute to anchorage-dependent growth (Howe, 2001), our data provide the first evidence that the PAK–Nck interaction serves as a regulatory step in PAK activation in adherent cells.

Basement membrane proteins promote PAK2 Ser-20 phosphorylation through enhanced eNOS activation and NO production (Figure 3). Whereas this work is the first to show that shear stress–induced eNOS activation is matrix specific, other groups have reported that matrix composition affects endothelial NO production. Specifically, González-Santiago *et al.* (2002) found that endothelial cells plated on the basement membrane component collagen IV produced more NO than cells on collagen I and this effect was integrin dependent. Viji *et al.* (2009) reported that endothelial cell attachment to fibronectin decreases eNOS gene expression and activity. Although we did not see a decrease in basal NO production or eNOS expression in endothelial cells on fibronectin, attachment to fibronectin significantly blunted shear stress–induced NO production, underscoring the importance of cell–matrix interactions in the endothelial response to shear. However, our data suggest that fibronectin diminishes NO production despite enhancing eNOS expression levels, potentially due to negative feedback of the NO/PKG pathway on NF-κB. Shear stress–induced eNOS expression requires NF-κB activation, and preventing NO production with L-NAME enhances both shear stress–induced NF-κB activation and eNOS expression (Grumbach *et al.*, 2005).

The signaling pathways upstream of eNOS activation are highly context and stimulus specific, with multiple signaling pathways implicated in shear stress–induced NO production. Although Akt represents the best-characterized signaling pathway upstream of eNOS, the current data suggest that Akt may play a larger role in eNOS phosphorylation by vascular endothelial growth factor (VEGF) than shear stress. Early work used phosphoinositide (PI) 3-kinase inhibitors and dominant-negative constructs to prove that Akt mediates shear-induced eNOS activation (Dimmeler *et al.*, 1999; Fulton *et al.*, 1999). However, PI 3-kinase inhibitors also block shear stress–induced integrin activation, suggesting that PI 3-kinase inhibitors may similarly block downstream activation of PKA in cells on basement membrane proteins (Orr *et al.*, 2007). Dominant-negative Akt blocks VEGF-induced eNOS phosphorylation but not shear stress–induced eNOS phosphorylation, whereas the PKA inhibitor H89 blocks shear stress–induced eNOS phosphorylation but not eNOS phosphorylation by constitutively active Akt (Boo *et al.*, 2002a). Overexpression of mutant Gab1 constructs independently inhibit either shear-induced Akt activation or eNOS phosphorylation, suggesting that the two pathways are not mechanistically coupled (Dixit *et al.*, 2005).

Endothelial NO production has both positive and negative effects on NF-κB–dependent proinflammatory gene expression. NF-κB promotes the expression of multiple NO synthase isoforms, including both eNOS and inducible NOS, and low levels of NO enhanced tumor necrosis factor α (TNFα)–induced NF-κB activation and inflammatory gene expression (De Caterina *et al.*, 1995; Khan
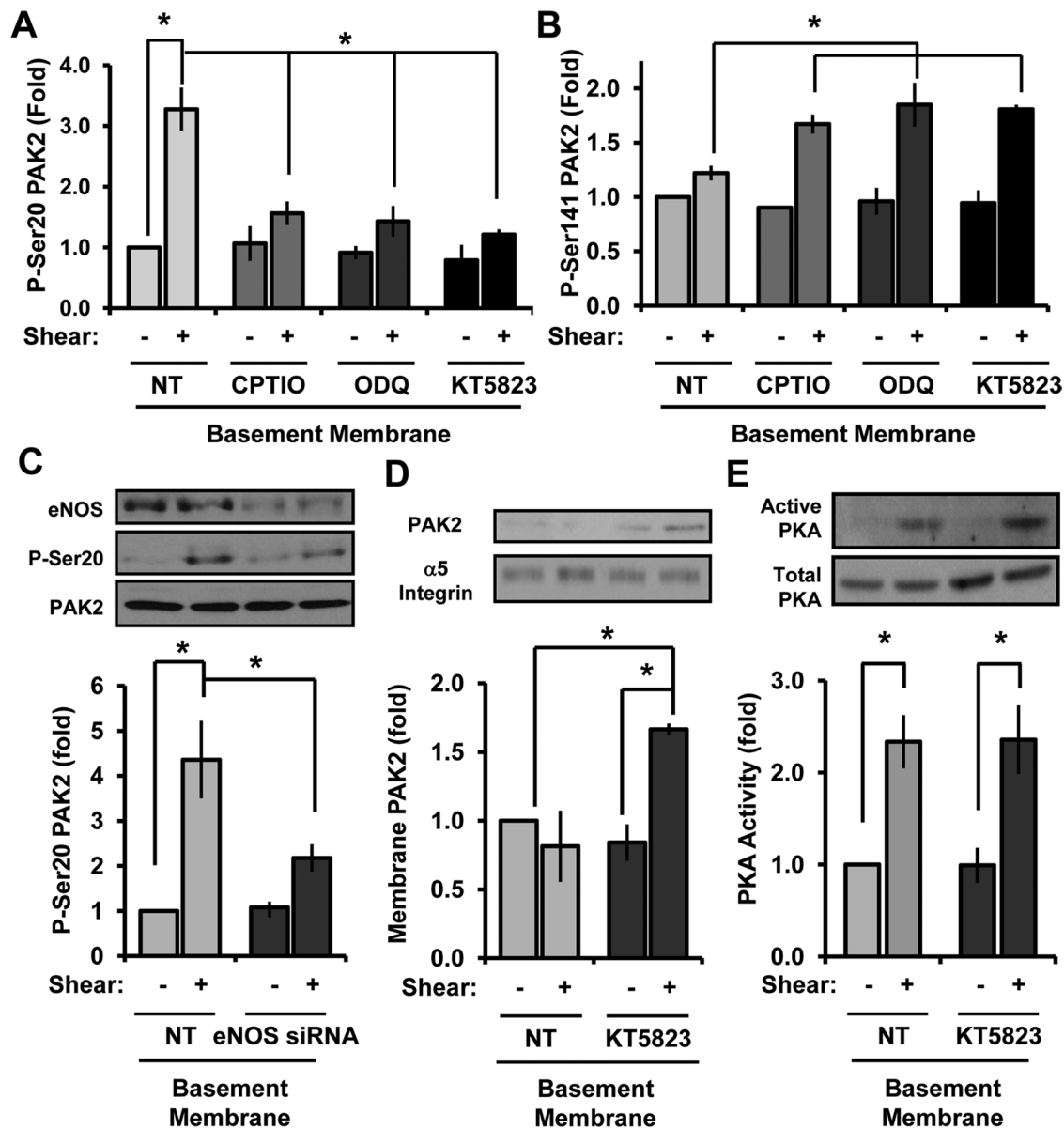
FIGURE 5: NO/PKG inhibitors blunt PAK2 Ser-20 phosphorylation and rescue PAK activation. (A) BAECs were left untreated (NT) or treated with CPTIO (200 µM, 30 min), ODQ (10 µM, 30 min), or KT5823 (2 µM, 1 h). Cells were sheared for 15 min, and Ser-20 phosphorylation was determined. $n = 4–7$. (B) Endothelial cells were treated as in A, and PAK2 Ser-141 phosphorylation was determined. $n = 3$. (C) Endothelial cells were transfected with eNOS siRNA, plated on BM, and exposed to shear stress for 15 min. Ser-20 phosphorylation was determined as previously described. $n = 3$. (D) Endothelial cells treated with KT5823 as in A were sheared for 15 min and PAK2 membrane translocation determined. Results are normalized to α5 integrin levels in the membrane fraction. Representative immunoblots are shown. $n = 3$. (E) Endothelial cells on BM were treated with KT5823 as in A and exposed to shear stress for 15 min. PKA activity was determined by affinity precipitation and normalized to total PKA in cell lysates. Values are means ± SE, $n = 3$. *$p < 0.05$.

et al., 1996; Umansky *et al.*, 1998). However, higher levels of NO can reduce both NF-κB DNA binding, an effect partially mediated by S-nitrosylation of Cys62 on the p50 subunit of NF-κB (Matthews *et al.*, 1996; Umansky *et al.*, 1998), and reduced degradation of the NF-κB inhibitor IκBα (Chen *et al.*, 1999a). In contrast to NO, only a few studies have linked protein kinase G signaling to inflammatory responses. Activation of cGMP/PKG signaling is not required for the inhibitory effect of NO on TNFα-induced NF-κB activation (Spiecker *et al.*, 1998); however, the mechanisms used by flow and TNFα to stimulate NF-κB differ substantially. PKG signaling was recently

found to inhibit diabetes-associated inflammation in both cell culture and animal model systems (Rizzo *et al.*, 2010; Lutz *et al.*, 2011), but the mechanisms by which PKG limits inflammation have not been determined. Our data suggest that NO and PKG mediate a portion of their anti-inflammatory effects through PKG-dependent PAK2 Ser-20 phosphorylation and inhibition of the PAK–Nck interaction.

Multiple recent reports illustrate a complex interaction between the Rac/PAK pathway and NO/PKG signaling. Rac1 haploinsufficient mice show reduced eNOS expression and activity and impaired vasodilation (Sawada *et al.*, 2008). Both treatment with a Rac1
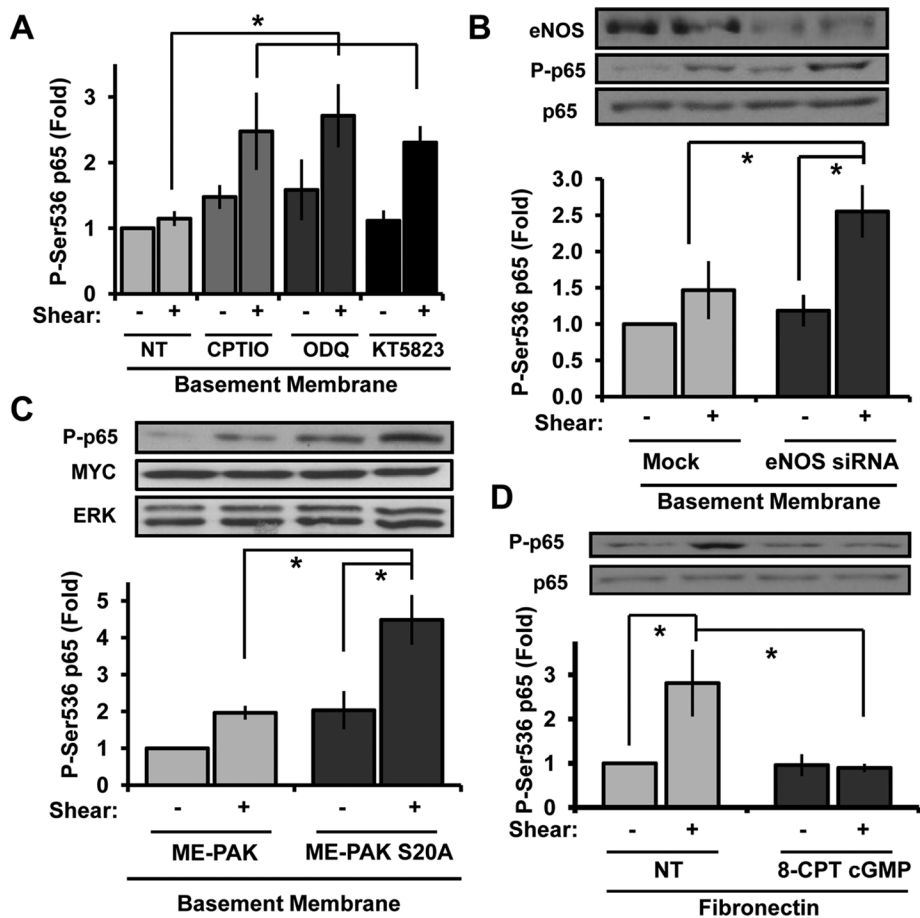
FIGURE 6: Inhibiting NO/PKG signaling rescues shear stress–induced NF-κB activation on basement membrane proteins. (A) BAECs were treated with CPTIO (200 μM, 30 min), ODQ (10 μM, 30 min), or KT5823 (2 μM, 1 h) and sheared for 30 min. NF-κB activation was determined by Western blotting cell lysates for p65 Ser-536 phosphorylation. Results were normalized to GAPDH, and values shown are means ± SE, $n = 3$. (B) Endothelial cells were transfected with eNOS siRNA, plated on basement membrane proteins, and exposed to shear stress for 15 min. p65 phosphorylation was determined as in A, $n = 3$. (C) Endothelial cells expressing ME-PAK2 or the mutant S20A ME-PAK2 were exposed to shear stress for 30 min, and NF-κB activation was determined as previously described. Representative Western blots are shown. $n = 3$. (D) Endothelial cells plated on fibronectin were treated with 8-CPT-cGMP (200 μM, 1 h), and shear stress–induced NF-κB activation was determined. Values are means ± SE, $n = 3$. *$p < 0.05$.

inhibitor and expression of dominant-negative Rac1 reduced eNOS mRNA transcription, as did expression of a dominant-negative PAK1 construct (K299R). Consistent with this, we found that shear stress–induced eNOS expression (but not activity) was enhanced in endothelial cells on fibronectin where PAK activity is highest (Supplemental Figure S4A). Rac1 stimulates transmembrane guanylate cyclase activation through a direct interaction of guanylate cyclase with active PAK1 or PAK2 in CHO cells (Guo et al., 2007). However, Rac/PAK signaling did not stimulate activation of NO-sensitive soluble guanylate cyclases in these experiments. Our data suggest that a novel negative feedback relationship exists between these two pathways, as Rac/PAK signaling promotes NF-κB–dependent eNOS expression, whereas eNOS-dependent NO production limits PAK activation by uncoupling the PAK–Nck interaction.

MATERIALS AND METHODS
Cell culture, transfection, and flow apparatus
Bovine aortic endothelial cells (BAECs) were cultured in DMEM containing 10% fetal bovine serum (FBS), 2 mM glutamine, 10 U/ml penicillin, and 10 μg/ml streptomycin (Gibco, Life Technologies, Carlsbad, CA) and were used between passages 6 and 12. HAECs were cultured in MCDB 131 containing 10% FBS, 2 mM glutamine, 10 U/ml penicillin, 10 μg/ml streptomycin (Gibco), 60 μg/ml heparin, and bovine brain extract (24 μg/ml) and were used between passages 6 and 10. Glass slides were coated with basement membrane extract (Matrigel, 1:50 dilution; BD Biosciences, San Diego, CA) or fibronectin (10 μg/ml) overnight at 4°C. Slides were then blocked in 0.2% denatured bovine serum albumin for 30 min. Cells were plated in low-serum-containing media (0.2–1.0% FBS) and exposed to onset of laminar flow (12 dynes/cm^2) or oscillatory flow (±5 dynes/cm^2 with 1 dyne/cm^2 superimposed) using parallel-plate flow apparatus with the environment maintained at 37°C and 5% CO$_2$ perfused into the system as previously described (Orr et al., 2005, 2008). H89 and PKI were purchased from Tocris Bioscience (Ellisville, MO), CPTIO was purchased from Sigma-Aldrich (St. Louis, MO), and ODQ was purchased from Cayman Chemical Company (Ann Arbor, MI). The ME-PAK2 construct (gift from Herma Renkema, University of Tampere, Tampere, Finland) underwent site-directed mutagenesis to change the serine 20 site to an alanine residue using the QuikChange II Site Directed Mutagenesis Kit according to manufacturer's protocol (Stratagene, Santa Clara, CA). BAECs were transfected with PKA Cα siRNA (10 nM for 24 h; Cell Signaling Technology, Beverly, MA), eNOS SMARTpool (25 nM for 48 h; Dharmacon, Lafayette, CO), ME-PAK2, and ME-PAK2 S20A using Lipofectamine 2000 (Invitrogen, Carlsbad, CA)).

Cytosol/membrane fractionation
To separate the cytosolic and membrane fractions, cells were washed once in ice-cold phosphate-buffered saline (PBS) and lysed in 250 μl of buffer containing 20 mM Tris, pH 7.5, 2 mM 2-mercaptoethanol, 5 mM ethylene glycol tetraacetic acid (EGTA), 2 mM EDTA, and 1× protease inhibitor cocktail (RPI, Mount Prospect, IL). Lysates were collected and spun for 30 min at 15,000 × g at 4°C. Supernatant was then collected as the cytosolic fraction. The remaining pellet was resuspended in 150 μl of buffer containing 50 mM Tris, pH 8.0, 150 mM NaCl, 1% NP-40, 10 mM NaF, 2 mM Na$_3$VO$_4$, and 1× protease inhibitor and spun for 30 min at 13,000 × g at 4°C. Supernatant was taken as the membrane fraction. Western blots were probed for PAK2, and the efficiency of fractionation was checked by blotting for α5 integrin (membrane fraction) and glyceraldehyde-3-phosphate dehydrogenase (GAPDH; cytosolic fraction).

Immunoblotting
Cell lysis and immunoblotting was performed as previously described (Orr et al., 2002). Antibodies used included rabbit anti–phospho-PAK2 (Ser-20), rabbit anti–NF-κB (p65 subunit, s536),
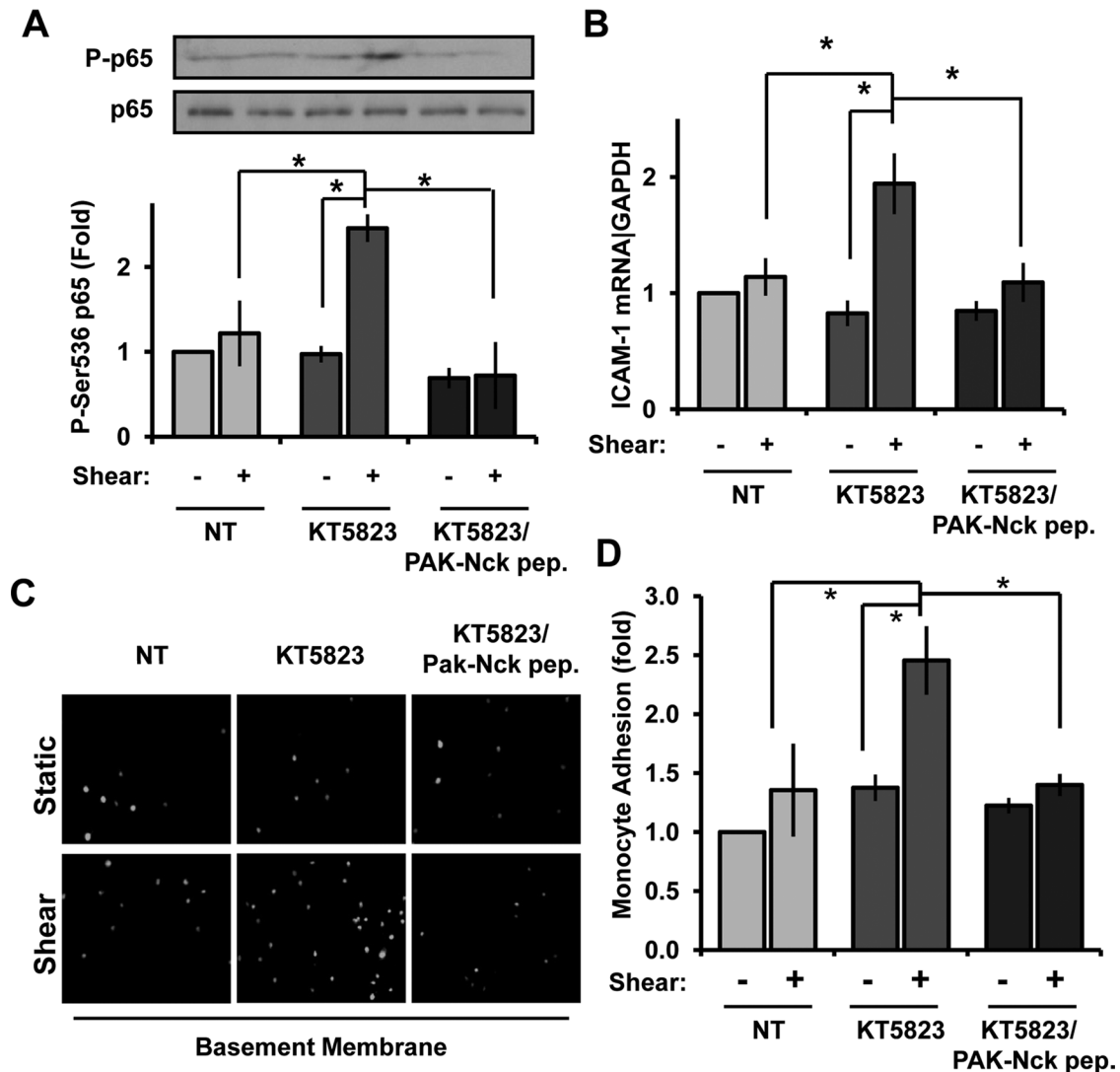
FIGURE 7: Blocking the PAK–Nck interaction prevents inflammatory signaling after PKG inhibition. (A) BAECs plated on basement membrane proteins were treated with KT5823 (2 µM) in either the absence or presence of the membrane-permeable, Tat-tagged PAK–Nck blocking peptide (20 µg/ml). Cells were then exposed to shear stress for 30 min, and NF-κB activation was determined. n = 3. (B) HAECs treated as in A were exposed to shear stress for 3 h to induce proinflammatory gene expression. ICAM-1 mRNA expression was determined by qRT-PCR and normalized to B2M mRNA levels. n = 3. *p < 0.05. (C) HAECs treated as in A were exposed to shear stress for 5 h, and the adhesion of Cell Tracker Green–labeled THP-1 monocytes was determined in static adhesion assays. Representative images are shown. (D) Monocyte adhesion in C was quantified by lysing cells in 100 mM NaOH and quantifying fluorescence in a plate reader. Results are normalized to total monocyte number (bound plus unbound) and expressed as a fold change compared with untreated cells under static conditions. Values are means ± SE, n = 3. *p < 0.05.

rabbit anti-PAK2, rabbit anti-PAK1/2/3 (Cell Signaling Technology), rabbit anti–phospho-PAK (Ser-141; Invitrogen), rabbit anti-ERK1/2, rabbit anti–PKA Cα, rabbit anti–phospho-PKA substrate, and mouse anti-Myc (Santa Cruz Biotechnology, Santa Cruz, CA). Densitometry was performed using ImageJ software (National Institutes of Health, Bethesda, MD).

Quantitative real-time PCR

mRNA was extracted using TRIzol (Invitrogen) per manufacturer's instructions, and cDNA was synthesized using the iScript cDNA synthesis kit (Bio-Rad, Hercules, CA). Quantitative real-time (qRT)-PCR was performed in a Bio-Rad iCycler using SYBR Green Master mix (Bio-Rad), and results were normalized to GAPDH or β2-microglobulin

using the 2ddCt method. Primer sequences are listed in Supplemental Table S1.

Immunoprecipitation and PAK kinase assay

Cells were lysed with immunoprecipitation lysis buffer (10 mM Tris, 150 mM NaCl, 1 mM EDTA, 1 mM EGTA, 10 mM NaF, 1% Triton X-100, 0.5% IGEPAL, 100 µM PMSF, and protease and phosphatase inhibitor cocktails [RPI]) and centrifuged at 15,000 rpm for 15 min at 4°C. Supernatant was incubated with either mouse anti-Myc antibody or rabbit anti-PAK2 overnight for 2 h (respectively) at 4°C. Gamma-bind G or protein A–Sepharose beads were incubated with supernatant for 2 h. Beads were pelleted by brief centrifugation and rinsed three times with lysis buffer. Immunoprecipitated
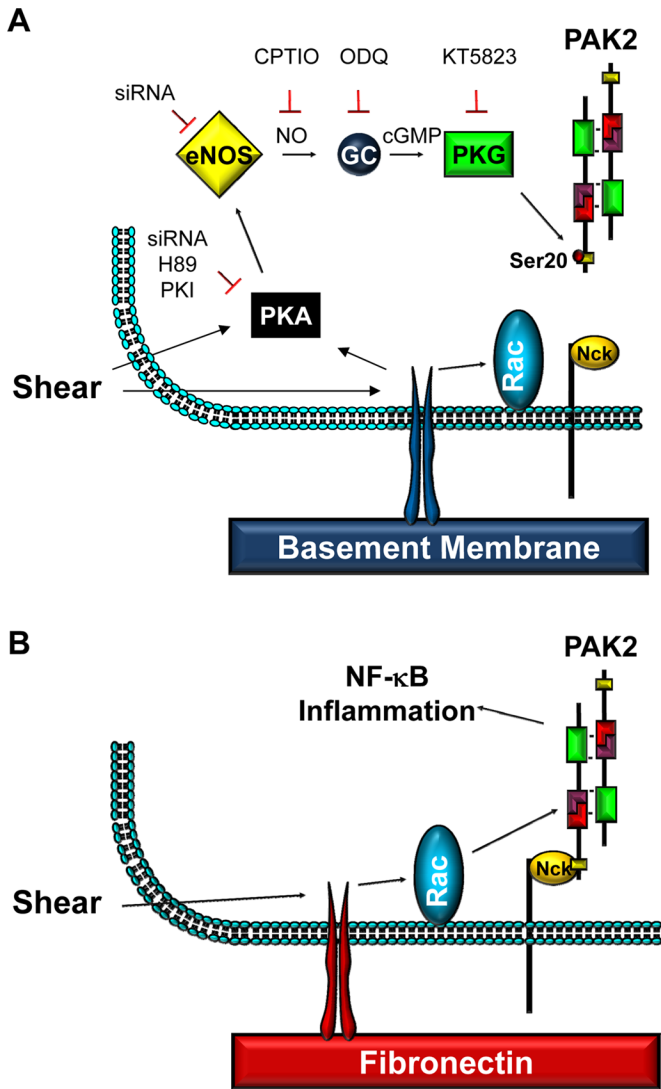
FIGURE 8: Model for PKG-mediated PAK2 Ser-20 phosphorylation and loss of PAK–Nck binding on basement membrane proteins.

proteins were recovered by resuspended the beads with 2× SDS sample buffer. ME-PAK2 expressed in BAECs was immunoprecipitated as previously described, and beads were washed twice with 500 μl of kinase reaction buffer (50 mM Tris, pH 7.4, 25 mM MgCl, 4 mM EGTA, 150 μM NaVO$_4$, 1 mM dithiothreitol, 500 μM ATP). After the final wash, 0, 1, and 5 ng of recombinant PKA catalytic subunit and 50 μl of kinase reaction buffer were added and incubated for 30 min at 30°C. Reactions were stopped by adding 20 μl of 6× Laemmli buffer. Samples were boiled at 95°C for 10 min, centrifuged at 15,000 rpm for 5 min, and stored at –20°C before analysis by Western blotting for phospho-PKA substrate and anti–phospho-PAK2 (Ser-20). Active PKA pull-down assays were performed as previously described using GST-PKI pseudosubstrate affinity pull downs (Paulucci-Holthauzen and O'Connor, 2006; Funk et al., 2010).

Nitric oxide species analysis

Reductive acidic triodiode (KI/I3)–based chemiluminescence was used on a Sievers NO analyzer to examine NOx concentrations in samples. Samples were lysed in a nitrite-preserving buffer (0.8 M K$_3$Fe(CN$_6$), 100 mM NEM, 10% NP-40). They were then injected into a purge vessel containing a solution with potassium iodide (66.8 mM), iodine (28.5 mM), and acetic acid (78% [vol/vol]). Signals were integrated and compared with sodium nitrite standard curves to calculate concentrations. Background levels of NOx were measured in all buffers and reagents, which were subtracted from sample NOx values and normalized to total protein.

Monocyte adhesion assay

Human THP-1 monocytes were labeled with Cell Tracker Green (Invitrogen) according to manufacturer's protocol. Monolayers of HAECs were treated as described, and (5.0–7.0) × 10^6 monocytes were added per shear stress slide. Monocytes were allowed to attach for 15 min at 37°C in Hank's balanced salt solution containing calcium and magnesium. Supernatant and two washes were collected as nonbound fraction in a microcentrifuge tube. Bound and nonbound monocytes were then lysed in 100 mM NaOH, and monocytes were quantified by measuring Cell Tracker Green fluorescence at 488 nm in a FLUOStar fluorescence plate reader. Results were normalized to unbound fraction and expressed as a fold change compared with untreated static cells.

Statistical analysis

Statistical comparisons between groups were performed using Prism software (GraphPad Software, La Jolla, CA), using Student's *t* test, one-way analysis of variance (ANOVA) with Newman–Keuls posttest, or two-way ANOVA with Bonferroni posttests. Error bars indicate SEs.

REFERENCES

Andrews AM, Jaron D, Buerk DG, Kirby PL, Barbee KA (2010). Direct, real-time measurement of shear stress-induced nitric oxide produced from endothelial cells in vitro. Nitric Oxide 23, 335–342.

Bokoch GM (2003). Biology of the p21-activated kinases. Annu Rev Biochem 72, 743–781.

Boo YC, Hwang J, Sykes M, Michell BJ, Kemp BE, Lum H, Jo H (2002a). Shear stress stimulates phosphorylation of eNOS at Ser(635) by a protein kinase A-dependent mechanism. Am J Physiol Heart Circ Physiol 283, H1819–H1828.

Boo YC, Sorescu G, Boyd N, Shiojima I, Walsh K, Du J, Jo H (2002b). Shear stress stimulates phosphorylation of endothelial nitric-oxide synthase at Ser1179 by Akt-independent mechanisms: role of protein kinase A. J Biol Chem 277, 3388–3396.

Boo YC, Sorescu GP, Bauer PM, Fulton D, Kemp BE, Harrison DG, Sessa WC, Jo H (2003). Endothelial NO synthase phosphorylated at SER635 produces NO without requiring intracellular calcium increase. Free Radic Biol Med 35, 729–741.

Chen F, Lu Y, Castranova V, Rojanasakul Y, Miyahara K, Shizuta Y, Vallyathan V, Shi X, Demers LM (1999a). Nitric oxide inhibits HIV tat-induced NF-kappaB activation. Am J Pathol 155, 275–284.

Chen ZP, Mitchelhill KI, Michell BJ, Stapleton D, Rodriguez-Crespo I, Witters LA, Power DA, Ortiz de Montellano PR, Kemp BE (1999b). AMP-activated protein kinase phosphorylation of endothelial NO synthase. FEBS Lett 443, 285–289.

Chiang HY, Korshunov VA, Serour A, Shi F, Sottile J (2009). Fibronectin is an important regulator of flow-induced vascular remodeling. Arterioscler Thromb Vasc Biol 29, 1074–1079.

Chiu JJ, Chien S (2012). Effects of disturbed flow on vascular endothelium: pathophysiological basis and clinical perspectives. Physiol Rev 91, 327–387.

De Caterina R, Libby P, Peng HB, Thannickal VJ, Rajavashisth TB, Gimbrone MA Jr, Shin WS, Liao JK (1995). Nitric oxide decreases cytokine-induced endothelial activation. Nitric oxide selectively reduces endothelial expression of adhesion molecules and proinflammatory cytokines. J Clin Invest 96, 60–68.

Dimmeler S, Fleming I, Fisslthaler B, Hermann C, Busse R, Zeiher AM (1999). Activation of nitric oxide synthase in endothelial cells by Akt-dependent phosphorylation. Nature 399, 601–605.

Dixit M, Loot AE, Mohamed A, Fisslthaler B, Boulanger CM, Ceacareanu B, Hassid A, Busse R, Fleming I (2005). Gab1, SHP2, and protein kinase A are crucial for the activation of the endothelial NO synthase by fluid shear stress. Circ Res 97, 1236–1244.

Fryer BH, Wang C, Vedantam S, Zhou GL, Jin S, Fletcher L, Simon MC, Field J (2006). cGMP-dependent protein kinase phosphorylates p21-activated kinase (Pak) 1, inhibiting Pak/Nck binding and stimulating Pak/vasodilator-stimulated phosphoprotein association. J Biol Chem 281, 11487–11495.

Fulton D, Gratton JP, McCabe TJ, Fontana J, Fujio Y, Walsh K, Franke TF, Papapetropoulos A, Sessa WC (1999). Regulation of endothelium-derived nitric oxide production by the protein kinase Akt. Nature 399, 597–601.

Funk SD, Yurdagul A, Green JM, Jhaveri KA, Schwartz MA, Orr AW (2010). Matrix-specific protein kinase A signaling regulates p21-activated kinase activation by flow in endothelial cells. Circ Res 106, 1394–1403.

González-Santiago L, López-Ongil S, Rodríguez-Puyol M, Rodríguez-Puyol D (2002). Decreased nitric oxide synthesis in human endothelial cells cultured on type I collagen. Circ Res 90, 539–545.

Grumbach IM, Chen W, Mertens SA, Harrison DG (2005). A negative feedback mechanism involving nitric oxide and nuclear factor kappa-B modulates endothelial nitric oxide synthase transcription. J Mol Cell Cardiol 39, 595–603.

Guo D, Tan YC, Wang D, Madhusoodanan KS, Zheng Y, Maack T, Zhang JJ, Huang XY (2007). A Rac-cGMP signaling pathway. Cell 128, 341–355.

Hahn C, Orr AW, Sanders JM, Jhaveri KA, Schwartz MA (2009). The subendothelial extracellular matrix modulates JNK activation by flow. Circ Res 104, 995–1003.

Hahn C, Schwartz MA (2009). Mechanotransduction in vascular physiology and atherogenesis. Nat Rev Mol Cell Biol 10, 53–62.

Howe AK (2001). Cell adhesion regulates the interaction between Nck and p21-activated kinase. J Biol Chem 276, 14541–14544.

Howe AK, Juliano RL (2000). Regulation of anchorage-dependent signal transduction by protein kinase A and p21-activated kinase. Nat Cell Biol 2, 593–600.

Khan BV, Harrison DG, Olbrych MT, Alexander RW, Medford RM (1996). Nitric oxide regulates vascular cell adhesion molecule 1 gene expression and redox-sensitive transcriptional events in human vascular endothelial cells. Proc Natl Acad Sci USA 93, 9114–9119.

Lu W, Katz S, Gupta R, Mayer BJ (1997). Activation of Pak by membrane localization mediated by an SH3 domain from the adaptor protein Nck. Curr Biol 7, 85–94.

Lu W, Mayer BJ (1999). Mechanism of activation of Pak1 kinase by membrane localization. Oncogene 18, 797–806.

Lutz SZ et al. (2011). Genetic ablation of cGMP-dependent protein kinase type I causes liver inflammation and fasting hyperglycemia. Diabetes 60, 1566–1576.

Matthews JR, Botting CH, Panico M, Morris HR, Hay RT (1996). Inhibition of NF-kappaB DNA binding by nitric oxide. Nucleic Acids Res 24, 2236–2242.

Orr AW, Hahn C, Blackman BR, Schwartz MA (2008). p21-activated kinase signaling regulates oxidant-dependent NF-kappa B activation by flow. Circ Res 103, 671–679.

Orr AW, Pallero MA, Murphy-Ullrich JE (2002). Thrombospondin stimulates focal adhesion disassembly through Gi- and phosphoinositide 3-kinase-dependent ERK activation. J Biol Chem 277, 20453–20460.

Orr AW, Sanders JM, Bevard M, Coleman E, Sarembock IJ, Schwartz MA (2005). The subendothelial extracellular matrix modulates NF-kappaB activation by flow: a potential role in atherosclerosis. J Cell Biol 169, 191–202.

Orr AW, Stockton R, Simmers MB, Sanders JM, Sarembock IJ, Blackman BR, Schwartz MA (2007). Matrix-specific p21-activated kinase activation regulates vascular permeability in atherogenesis. J Cell Biol 176, 719–727.

Paulucci-Holthauzen AA, O'Connor KL (2006). Use of pseudosubstrate affinity to measure active protein kinase A. Anal Biochem 355, 175–182.

Rizzo NO, Maloney E, Pham M, Luttrell I, Wessells H, Tateya S, Daum G, Handa P, Schwartz MW, Kim F (2010). Reduced NO-cGMP signaling contributes to vascular inflammation and insulin resistance induced by high-fat feeding. Arterioscler Thromb Vasc Biol 30, 758–765.

Rohwedder I, Montanez E, Beckmann K, Bengtsson E, Duner P, Nilsson J, Soehnlein O, Fassler R (2012). Plasma fibronectin deficiency impedes atherosclerosis progression and fibrous cap formation. EMBO Mol Med 4, 564–576.

Sawada N, Salomone S, Kim HH, Kwiatkowski DJ, Liao JK (2008). Regulation of endothelial nitric oxide synthase and postnatal angiogenesis by Rac1. Circ Res 103, 360–368.

Spiecker M, Darius H, Kaboth K, Hubner F, Liao JK (1998). Differential regulation of endothelial cell adhesion molecule expression by nitric oxide donors and antioxidants. J Leukoc Biol 63, 732–739.

Umansky V, Hehner SP, Dumont A, Hofmann TG, Schirrmacher V, Droge W, Schmitz ML (1998). Co-stimulatory effect of nitric oxide on endothelial NF-kappaB implies a physiological self-amplifying mechanism. Eur J Immunol 28, 2276–2282.

Viji RI, Kumar VBS, Kiran MS, Sudhakaran PR (2009). Modulation of endothelial nitric oxide synthase by fibronectin. Mol and Cell Biochem 323, 91–100.

Zhan Q, Ge Q, Ohira T, Van Dyke T, Badwey JA (2003). p21-activated kinase 2 in neutrophils can be regulated by phosphorylation at multiple sites and by a variety of protein phosphatases. J Immunol 171, 3785–3793.

Zhao ZS, Manser E, Lim L (2000). Interaction between PAK and nck: a template for Nck targets and role of PAK autophosphorylation. Mol Cell Biol 20, 3906–3917.

Zhou G-L, Zhuo Y, King CC, Fryer BH, Bokoch GM, Field J (2003). Akt phosphorylation of serine 21 on Pak1 modulates Nck binding and cell migration. Mol Cell Biol 23, 8058–8069.